

Ensemble Effect Evidenced by CO Adsorption on the 3-Fold PdGa Surfaces

Jan Prinz,^{†,‡} Roberto Gaspari,^{†,§} Quirin S. Stöckl,^{||} Peter Gille,[⊥] Marc Armbrüster,[#] Harald Brune,[‡] Oliver Gröning,[†] Carlo A. Pignedoli,[†] Daniele Passerone,[†] and Roland Widmer^{*,†}

[†]Empa, Swiss Federal Laboratories for Materials Science and Technology, nanotech@surfaces Laboratory, Ueberlandstrasse 129, 8600 Dübendorf, Switzerland

^{||}Empa, Swiss Federal Laboratories for Materials Science and Technology, Nanoscale Materials Science, Ueberlandstrasse 129, 8600 Dübendorf, Switzerland

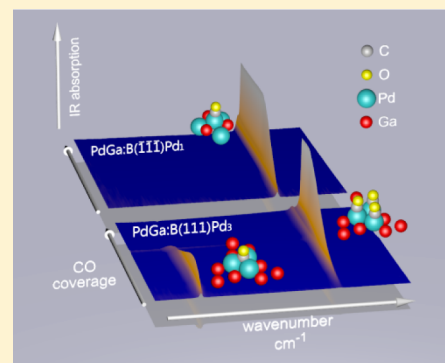
[⊥]Dept. für Geo- und Umweltwissenschaften, Ludwig-Maximilians-Universität, 80333 München, Germany

[#]Max-Planck-Institut für Chemische Physik fester Stoffe, 01187 Dresden, Germany

[‡]Institute of Condensed Matter Physics, Station 3, Ecole Polytechnique Fédérale de Lausanne (EPFL), 1015 Lausanne, Switzerland

Supporting Information

ABSTRACT: The atomic structure and composition of a catalyst's surface have a major influence on its performance regarding activity and selectivity. In this respect, intermetallic compounds are promising future catalyst materials, as their surfaces exhibit small and well-defined ensembles of active metal atoms. In this study, the active adsorption sites of the 3-fold-symmetric surfaces of the PdGa intermetallic compound were investigated in a combined experimental and computational approach using CO as a test molecule. The PdGa(111) and $(-1-1-1)$ surfaces exhibit very similar electronic structures, but have Pd sites with very different, well-defined atomic coordination and separation. They thereby serve as prototypical model systems for studying ensemble effects on bimetallic catalytic surfaces. Scanning tunneling microscopy and Fourier transform infrared spectroscopy show that the CO adsorption on both surfaces is solely associated with the topmost Pd atoms and Ga acts only as an inactive spacer. The different local configurations of these Pd atoms dictate the CO adsorption sites as a function of coverage. The experimental results are corroborated by density functional theory and illustrate the site separation and ensemble effects for molecular adsorption on intermetallic single crystalline surfaces.



1. INTRODUCTION

Surface science methods allow for studying the structure of catalytic surfaces on the atomic level, and in some cases even under reaction pressures.^{1,2} This ability expanded the understanding of heterogeneous catalysis and led to many ideas on how to structure catalyst surfaces to improve their performance.^{3–6} An important aspect of research in catalysis, besides achieving high activity, is improving selectivity. One proposed enhancement is the dilution of the active (metal) species with less active spacer atoms. This site isolation concept consists of forming isolated catalytic centers of reduced size, leading to a limited number of adsorption configurations for the reactants, which is called the “ensemble effect”.^{7–9} The number of reaction pathways emerging from these active centers is thereby reduced, resulting in an increased selectivity, as compared to metal surfaces consisting of a single element.

In addition to this ensemble effect, the electronic structure of the active species is influenced by the nature and concentration of the spacer atoms, which is known as the “ligand effect”.^{7,9} Since atomic and electronic structure of a surface are always interconnected, it is difficult to unambiguously impute a given

experimental observation purely to the ligand-, and/or to the ensemble effect of a catalytic surface.

One model system in this respect is bimetallic surface alloys, which have a random spatial distribution of active sites.^{3,7–11} Intermetallic compounds (IMCs) are a second model system, which have an ordered crystal structure. Additionally, they exhibit a higher energy of formation, which potentially increases surface stability.^{3,10–12} In this respect, the PdGa IMC has recently received considerable interest due to its high activity, stability, and selectivity in the semihydrogenation of acetylene.^{12,13} This reaction is industrially important,¹⁴ as it is a crucial step in polyethylene production, where currently Ag–Pd alloy catalysts are applied. In the context of the site isolation concept, also for PdGa, Pd is supposed to take the role of the catalytically active species and Ga the role of the spacer atom.

In a recent publication,¹⁵ we reported on the 3-fold surfaces of the PdGa IMC. The two crystallographically opposed

Received: February 13, 2014

Revised: May 14, 2014

Published: May 14, 2014

surfaces, (111) and $(-1-1-1)$, exhibit equal surface symmetry, equal lattice parameters, and very similar electronic structure, but different atomic configurations of the Pd atoms. On one surface separated Pd trimers are present, while the other is terminated by isolated, single Pd atoms. This particular situation allows for investigating the pure structural ensemble effect, while the influences from the ligand effect can be neglected.

On the other hand, studying the ligand effect can be accomplished by exchanging the chemical species of the spacer atoms, while keeping the atomic surface structure unchanged. Whereas the realization of this concept is experimentally challenging, it has been used in theoretical studies, such as in quantum chemical calculations performed by Nørskov et al.¹⁶ This computational screening for improved catalysts reveals trends for the selection of the most promising constituent materials.

In this study, we present experimental and computational results of CO adsorption on the PdGa:B $(-1-1-1)$ Pd₁ and PdGa:B(111)Pd₃ surfaces.¹⁵ These two surfaces serve as prototypical system to study the ensemble effect because they expose two different terminations. One consisting of single palladium atoms (Pd₁) and the second of palladium trimers (Pd₃). The effects of the Pd site structure are directly observed in the vibrational frequency of the adsorbed CO as a function of coverage as measured by Fourier transform infrared spectroscopy (FTIR). Scanning tunneling microscopy (STM) provides local information on the adsorption geometry and allows an unambiguous interpretation of the vibrational spectroscopy. Density functional theory (DFT) calculations agree with the experimental results and allow for an in depth understanding of the bonding situation of CO to the single atomic and trimer Pd sites.

We observe strong site isolation effects on both PdGa surfaces, which are most clearly expressed on the PdGa:B $(-1-1-1)$ Pd₁ surface, where the full CO coverage at low-temperature (77 K) and pressure (10^{-6} mbar range) is about 15% of that of Pd(111). To the best of our knowledge, this is the first experimental demonstration of the ensemble effect on well-defined intermetallic compound surfaces, which is a promising class of materials for the development of future catalysts.

2. METHODS

Experiments. The growth and surface preparation of the PdGa single crystals has been described in detail previously, so that only a brief summary is given.^{17,18} The PdGa single crystal surfaces were cleaned by Ar-ion sputtering and high temperature annealing (870 K) cycles.^{15,19} The STM measurements were performed with an Omicron low-temperature (LT-) STM at a base pressure below 5×10^{-11} mbar using a mechanically cut Pt/Ir-tip.

FTIR absorption spectroscopy measurements were recorded with a Bruker Vertex 70v/80v spectrometer in reflection-absorption mode (RAIRS). CO (purity 4.7, CANGas) was dosed on the sample at 90 K (± 10 K) by backfilling the main chamber.

Simulations. All simulations were performed within DFT in the mixed Gaussian Plane Waves framework as implemented in the CP2K code (see SI for further details).²⁰ We used the Perdew–Burke–Ernzerhof (PBE)²¹ parametrization for the exchange correlation functional.

PdGa slabs were simulated in the repeated slab geometry.²² Orthorhombic simulation cells of 23 and 24 atomic PdGa layers were used for simulations of the PdGa:B(111) and PdGa:B $(-1-1-1)$ surface, respectively. The positions of the lowest eight layers were fixed in the structure optimization. About 3 nm of vacuum was added above the adsorbate atoms. The lateral dimension of the cell corresponds to 12 hexagonal surface unit cells. The ground state adsorption energies and structures were computed by relaxing all atomic positions until forces were lower than 0.05 eV/nm. IR spectra were calculated using finite differences starting from the equilibrium adsorption geometries.²⁰

3. RESULTS AND DISCUSSION

A first approach to determine the adsorption sites of CO on PdGa:B(111)Pd₃ and $(-1-1-1)$ Pd₁ was performed by LT-STM measurements. Figure 1 shows STM images of both

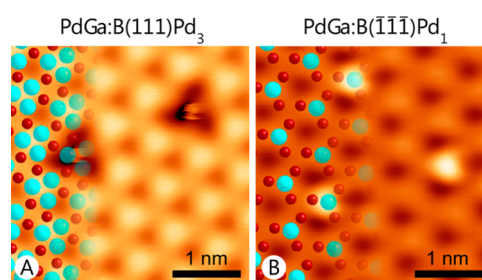


Figure 1. STM images of CO adsorbed on Pd₃ (A) and Pd₁ (B). The atomic surface structure is overlaid on the left-hand side of each image (Pd: cyan, large; Ga: red, small). The top layer consists of Pd trimers, for Pd₃ (A), and single Pd atoms for Pd₁ (B). The second layer consists of Ga trimers for both surface orientations. On Pd₃ (A), two CO molecules are present, appearing as triangular depressions. On Pd₁ (B), three CO molecules are present, appearing as protrusions (Tunneling parameters: A: -7 mV, 2 nA; B: -1 V, 35 nA).

surfaces at very low CO coverage. The surface Pd atoms are imaged as protrusions.¹⁵ In combination with low energy electron diffraction (LEED) measurements and STM simulations, the atomic structure of the clean surface is identified with regard to lateral position and orientation,¹⁵ and overlaid on the left-hand side of each image for the two surfaces. The samples were exposed to CO during imaging at 78 K, which allowed for identifying single adsorbed CO molecules. On Pd₃, CO molecules appear as triangular depressions with a central maximum, whereas on Pd₁, they are imaged as bright protrusions. According to the atomic structure overlay, individual CO molecules adsorb in the 3-fold Pd hollow site on Pd₃, and at the on-top Pd site on Pd₁.

To complement these atomic scale observations and to study the adsorption kinetics, RAIRS experiments as a function of CO coverage were carried out. As shown in Figure 2, a single, CO coverage independent, absorption peak is observed for the Pd₁ surface. For the Pd₃ surface, two separate, coverage dependent peaks are observed. Comparison of the peak positions with RAIRS of CO on Pd(111) allows for an assignment of the peaks at higher and lower wavenumbers found for CO/Pd₃ to on-top and hollow site adsorption, respectively.^{3,23} This assignment is substantiated by the sequence of binding energies of the optimized adsorption configurations found by DFT for adsorption of one, two, and three CO per Pd trimer (see Table 1 and Supporting

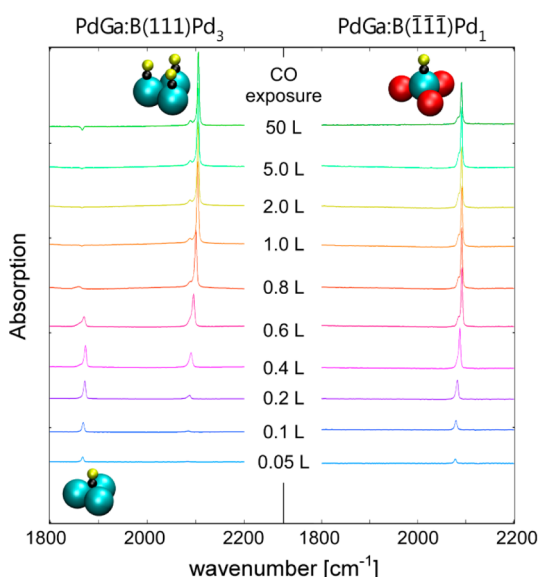


Figure 2. IR absorption spectra as a function of wavenumber and CO exposure at 90 K on Pd₃ (left) and Pd₁ (right). Insets next to the peaks show the respective adsorption configuration (C in black, O in yellow).

Information). Therefore, the series of RAIRS spectra for the CO/Pd₃ can be interpreted as a transition from hollow to on-top site with increasing exposure.^{3,23} A qualitative comparison to similar experiments of CO/Pd(111) reveals that peak shapes are sharper and coverage-dependent peak shifts are much smaller for the CO/PdGa system presented here. Indeed, on

Table 1. Experimental and Theoretical IR Absorption Peak Positions for CO on the Different Sites of the PdGa Surfaces and Calculated Binding Energies^a

| | CO/Pd ₃ (hollow site) | CO/Pd ₃ (on-top site) | CO/Pd ₁ (on-top site) |
|--|-------------------------------------|-------------------------------------|-------------------------------------|
| ν_{exp} (cm ⁻¹) | 1868–1874 | 2084–2105 | 2078–2092 |
| ν_{th} (cm ⁻¹) | 1822 | 2039 (2 CO) 2047 (3 CO) | 2032 |
| E_{b}/CO (eV) | 1.59 | 1.28 (2 CO) 1.25 (3 CO) | 1.37 |
| Pd–C bond order | 1.34 (3 × 0.45) | 0.82 | 0.83 |
| C–O bond order | 0.91 | 0.98 | 0.95 |

^aThe covalent bond orders are computed according to Angyan.²⁹ For a CO molecule in the gas phase the theory predicts a value of 1.51, accounting for the polar character of the C–O bond (2.89 for the covalent triple bond in C₂H₂).

CO/Pd(111), a full hierarchy of bonding sites is observed (hollow, bridge, and on-top sites), with a coverage-dependent spectrum influenced by long-ranged intermolecular interactions,^{23–25} leading to broadened IR-absorption features. Accordingly, our RAIRS data clearly indicates a suppression of CO–CO interactions on both PdGa surfaces. This is most pronounced in the CO/Pd₁ case, where the on-top sites are separated by 0.69 nm, but is also seen for CO/Pd₃, where at full coverage, the interaction is mainly reduced to the three neighboring CO molecules on the same trimer. Additionally, the Pd–Pd nearest neighbor distance of 0.3 nm within such a Pd trimer is 10% larger than in Pd(111).¹²

A summary of the experimental IR vibration frequencies is shown in Table 1, together with simulated frequencies from DFT for the most stable adsorption geometries, which corroborate the experimental vibrational assignments. The ranges given for the experimental frequencies represent the coverage-dependent variations in peak positions. The computed vibration frequencies underestimate the experimental values by a constant scaling of $2.80 \pm 0.02\%$. This is a common problem in DFT with PBE approximation (see refs 11 and 26) and can vary according to the parametrization employed.²⁷ However, the agreement of the relative frequencies by less than 0.5% confirms the hypothetical structure model used in DFT.

The combined experimental and theoretical data enables us to interpret the CO/PdGa(111) and (–1–1–1) systems as follows: On Pd₃, the adsorption site is coverage dependent, the 3-fold hollow site is occupied at low coverage, and the on-top site is occupied if two or three CO are present on one Pd trimer. Pd₁ allows only for on-top adsorption on the terminating Pd atom. According to DFT, in all CO binding conformations the molecular axis is oriented perpendicular to the surface (see insets in Figure 2).

Along with this interpretation, details in the RAIRS results shown in Figure 2 can be explained. The frequency shift from initial to full coverage of the peaks originating from on-top site species amounts to 14 cm⁻¹ for CO/Pd₁ and 21 cm⁻¹ for CO/Pd₃. The full coverage is obtained after exposure to 0.6 and 1.2 L for Pd₁ and Pd₃, respectively. On Pd₁, the shift is assigned to interactions with the nearest neighbor adsorbates (1–6 CO) separated by 0.69 nm. For CO adsorbed at the on-top site on Pd₃, the main contribution to the shift is attributed to the occupancy increase from two to three CO per trimer at a mutual distance of 0.31 nm.

Both on-top site peaks exhibit a shoulder at lower wavenumbers, which for CO/Pd₁ shifts along with the main peak, but for CO/Pd₃, remains at a fixed position. These side peaks are assigned to CO molecules neighboring, for example, a surface vacancy¹⁵ or a step edge.²⁸

The coverage-dependent transition from hollow to on-top site adsorption and the small vibrational shifts due to weak CO–CO interactions are in agreement with high resolution electron energy loss spectroscopy (HREELS) of CO adsorbed on PdAg surface alloys of different Pd concentrations.¹⁰

Additionally, the CO binding energies shown in Table 1 are comparable to those computed for PdAg/Pd(111) surface alloys.¹¹ Using the same PBE functionals, Mancera et al.¹¹ found on-top site binding energies of 1.37 and 1.29 eV for CO on single Pd atoms and trimers, respectively. These energies are in very good agreement with our calculations (1.37 and 1.25 eV) for PdGa. On the other hand, the hollow site adsorption energy deviates with 1.97 eV for PdAg from the value of 1.59 eV found for PdGa. This difference might be a consequence of the reduced Pd–Pd distance in the trimer of the surface alloy, and/or of the different ligand effects of Ag and Ga.

To get a broader insight into the adsorption energy landscape, the binding energies for other possible sites were calculated using DFT. A summary of all tested configurations is given in the Supporting Information. On Pd₁, the trimers of Pd atoms, lying 143 pm below the Pd₁ termination, are found less favorable for CO adsorption ($E_{\text{b}} = 0.88$ eV), since the atoms of this third-outermost layer are almost completely coordinated with bulk atoms. Furthermore, CO adsorbed on the hollow site of the Ga trimers of the second-outermost layer (53 and 56 pm below the surface layer on Pd₃ and Pd₁, respectively) was

computed to have a weaker binding energy on both terminations ($E_b = 0.08$ eV for Pd₃ and 0.56 eV for Pd₁). To investigate the absence of CO bridge site bonding on Pd₃, the binding energies for two CO molecules in “top-and-bridge” and “top-and-top” configuration on the Pd trimer were computed. For both situations, a local energetic minimum was found, with the “top-and-top” configuration being preferred by 63 meV per CO molecule. A single molecule located on the trimer in a Pd–Pd bridge site was found unstable in the DFT optimization. The large relative differences in binding energies between the first and the second preferred adsorption sites found by DFT confirms the experimental observation that both surfaces exhibit saturation after adsorption of one and three CO molecules per surface unit cell, respectively.

Krajci and Hafner conducted a computational study on the structure and adsorption properties of the 3-fold PdGa surface.³⁰ Their adsorption energies for CO on the Pd₁ and Pd₃ surface are in agreement with our DFT derived values summarized in Table 1, with a shift to lower binding energies, which is consistent with the different parametrization for the PBE approximation. However, in their study they concluded Ga surface terminations to be energetically more favorable than the Pd ones, which we find to be incompatible with experiment (see Supporting Information).^{15,19}

We studied the coverage dependence for CO/Pd₃ in more detail by LT-STM. Images at higher coverage than in Figure 1 reveal four different CO occupations per Pd-trimer, namely, one, two, three, and no CO molecules per trimer (cf. Figure 3). As already shown in Figure 1, we find that one CO per Pd trimer appears as a single protrusion that is centered on the Pd₃ trimer. If two CO molecules are adsorbed on a Pd trimer, the imaged adsorbate has a larger apparent height and an elliptical shape (Figure 3A). The center of the protrusion is found slightly off the Pd₃ hollow sites located at the intercepts of the red grid (Figure 3B). Additionally, their long semiaxis is not oriented along the $\langle 1-10 \rangle$ directions, but along the lines connecting two of the three Pd atoms in the trimer. The sketch in Figure 3C shows the orientation of trimers as determined by LEED-I(V).¹⁵ Together with the change in IR-absorption frequency, we conclude that adding one more CO molecule per Pd₃ converts the 3-fold hollow site to three on-top sites of which two are occupied. Higher coverage leads to wider, 3-fold symmetric protrusions (Figure 3D), exhibiting the same orientation as the Pd₃ trimers, which is consistent with the hypothesis of three CO molecules in the on-top site configuration on the topmost Pd atoms. Accordingly, STM confirms on a local scale the adsorption site sequence derived from RAIRS and DFT simulations for CO/Pd₃. As seen from the STM topographies for CO on Pd₃ and Pd₁, shown in Figures 1 and 3, CO molecules are found exclusively at the positions of the protrusions on the clean surfaces. As these protrusions coincide with the outermost Pd atoms,¹⁵ we find no indication for bonding of CO to Ga.

The presented data show different expression of the active site separation on the Pd₃ and Pd₁ terminations. At low coverage, the adsorption sites have the same separation on both surfaces (one CO per unit cell), but are of a different type, namely, on-top site for Pd₁ and hollow site for Pd₃. However, the Pd₃ surface also has three adjacent Pd on-top adsorption sites that are populated at high coverage; therefore it can accommodate three times as many CO than the Pd₁ surface. This means that at full CO coverage the minimum CO–CO

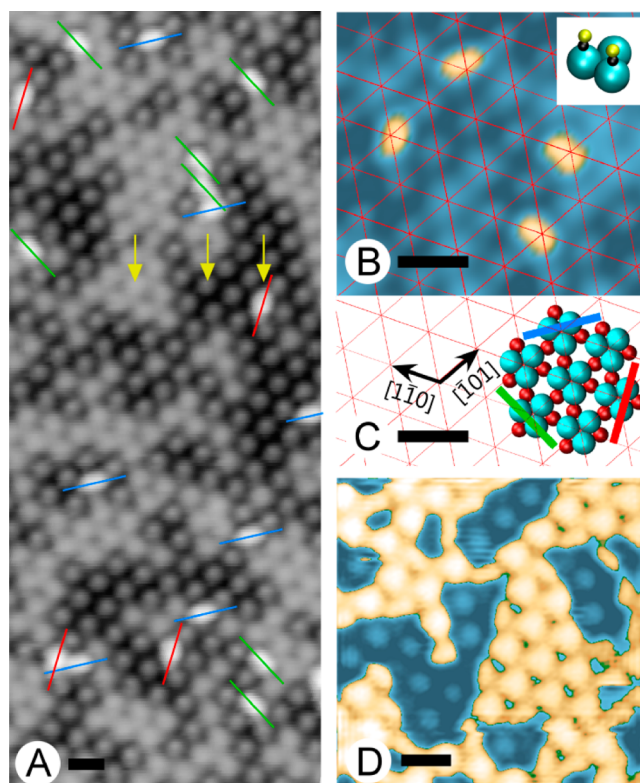


Figure 3. (A) LT-STM image of a partially CO covered PdGa-B(111)-Pd₃ surface. A Pd₃ trimer with no CO (left arrow) appears in light-gray. A trimer with one CO (center arrow) appears as a well localized protrusion with lower apparent height, and a trimer with two CO (right arrow) as elongated white protrusion. The different elongated protrusions appear in three distinct directions indicated by the colored lines. These directions coincide with the “edges” of a Pd trimer (see C). (B) Detail showing that elliptical protrusions are off center with respect to the Pd₃ lattice. (C) Surface atomic structure derived from LEED-I(V).¹⁵ (D) Increased CO exposure leads to protrusions with triangular envelopes, that is, fully occupied trimers. Scale bars correspond to 1.0 nm. In B and C, a different color-scale was chosen to emphasize the shape of the CO protrusions (beige; tunneling parameters: (A, B) 0.2 V, 0.5 nA; (D) –2.5 V, 0.5 nA).

separation is 0.69 nm for the Pd₁ surface and only 0.31 nm for the Pd₃ surface.

To investigate the chemical behavior of the active sites we characterized the nature of the binding of CO to the Pd sites by computing the covalent bond-order index, following the approach by Angyan et al.²⁹ in the framework of Bader’s topological theory. The method is basis-set independent and takes into account bond ionicities, leading to reduced bond orders for polar covalent bonds. For CO adsorbed on PdGa, the computed covalent Pd–C bond order reveals that the bonding character in the case of one CO molecule per surface unit cell is remarkably different on the two surfaces, whereas the on-top site bond configuration for high coverage is very similar. In the Pd₁ case, our analysis indicates a bond order of 0.83 for the Pd–C bond (where a value of 2.89 would correspond to C–C triple bond, as in acetylene). In the Pd₃ case, when CO is adsorbed at the hollow site of the trimer, each Pd atom contributes a bond order of 0.45, for a total bond order of 1.34. Indeed, the calculated adsorption energy in this configuration is higher compared to Pd on-top and the IR active CO vibrational mode has a lower frequency due to the weakened C–O bond, which is indicated by a small reduction

of the C–O covalent bond order (cf. Table 1). In the case of three CO per Pd₃, the situation is again similar to CO on Pd₁, which is reflected in binding energy, vibrational mode frequency and a comparable bond-order of 0.82 and 0.83, respectively.

For both 3-fold PdGa surfaces the site isolation concept is realized for the CO adsorption. This can be seen in particular by comparing it to CO adsorption on Pd(111). In the case of the Pd₁ surface, full CO coverage is obtained at a much lower molecular density of 2.41 CO/nm² compared to 15.26 CO/nm² for Pd(111), with both cases having on-top Pd adsorption. In the case of the Pd₃ surface the CO adsorption proceeds from hollow site adsorption on the Pd trimer to on-top site adsorption with increasing coverage, reaching a maximum CO density of 7.23 CO/nm². Although the CO density on the Pd₃ surface is a factor of 2 lower compared to Pd(111), the nearest CO–CO distance is only 10% different (Pd₃, 0.31 nm; Pd(111), 0.275 nm). The reason for the very different molecular saturation densities is the large separation between the trimers on Pd₃. While the local Pd trimers on Pd₃ do not show bridge site adsorption for CO, this is observed on Pd(111). Therefore, Pd(111) exhibits an almost continuous transition from hollow to bridge to on-top site adsorption with increasing coverage.^{23,24}

This transition was also reported for Pd ensembles on PdAu and PdAg surface alloys.^{3,8,10} In these alloys, the Pd ensemble size depends on the random local Pd concentration at the surface, whereas in the PdGa (111) and (–1–1–1) surfaces, size and separation are given by the crystal structure and do not allow for CO bridge site adsorption. However, the Pd ensembles found in the partially covalently bound IMC retain their adsorption properties, as adsorption sites, energy, and vibrational modes compare for CO adsorbed on the IMC and on the surface alloys, for Pd ensembles of equal size.

4. CONCLUSIONS

We compared the two 3-fold-symmetric surfaces of the PdGa IMC with regard to active adsorption site separation and ensemble effect. CO was used as a test molecule, confirming the active site isolation¹² and revealing differences in the ensemble effect for the two surface structures exhibiting single atoms (Pd₁) and trimers (Pd₃). Our combined analysis of STM, RAIRS, and DFT shows that Pd₁ provides, independent of coverage, only one on-top site for CO, whereas Pd₃ allows for hollow site adsorption at low coverage and on-top site adsorption at high coverage. This leads to a maximum occupancy of one and three CO molecules per surface unit cell for Pd₁ and Pd₃, respectively, while no adsorption is taking place on Ga related sites. This observation underlines the hypothesis that the Ga indeed only assumes the role of a spacer atom with regard to the CO adsorption properties.

Due to the similar electronic structure of these surfaces, the differences in their bonding properties are mainly attributed to the geometric ensemble effect. Furthermore, the comparison with CO adsorption studies on Pd-containing surface alloys supports the argument of a dominating ensemble- over the ligand effect in this IMC. This concept of the ensemble effect in PdGa combined with the active site isolation represents a paradigm for the study of selective catalytic reactions.

■ ASSOCIATED CONTENT

Supporting Information

Data on STM topography contrast of CO, details on the computations, and a verification of the PdGa:B(111)Pd₃ and PdGa:B(–1–1–1)Pd₁ surface structures with respect to ref 30. This material is available free of charge via the Internet at <http://pubs.acs.org>.

■ AUTHOR INFORMATION

Corresponding Author

*E-mail: roland.widmer@empa.ch. Tel.: +41 58 765 4745.

Present Address

[§]Drug Discovery and Development, Italian Institute of Technology, Via Morego 30, 16163 Genova, Italy (R.G.).

Notes

The authors declare no competing financial interest.

■ ACKNOWLEDGMENTS

We gratefully acknowledge funding by the Swiss National Science Foundation under Contract 200021-129511 and support by the Swiss National Supercomputing Center (CSCS).

■ REFERENCES

- (1) Bocklein, S.; Gunther, S.; Wintterlin, J. High-Pressure Scanning Tunneling Microscopy of a Silver Surface During Catalytic Formation of Ethylene Oxide. *Angew. Chem., Int. Ed.* **2013**, *52*, 5518–5521.
- (2) Herbschleb, C. T.; Bobaru, S. C.; Frenken, J. W. M. High-Pressure STM Study of NO Reduction by CO on Pt(100). *Catal. Today* **2010**, *154*, 61–67.
- (3) Chen, M. S.; Kumar, D.; Yi, C. W.; Goodman, D. W. The Promotional Effect of Gold in Catalysis by Palladium-Gold. *Science* **2005**, *310*, 291–293.
- (4) Somorjai, G. A. Surface Science and Catalysis. *Science* **1985**, *227*, 902–908.
- (5) Ertl, G.; Freund, H. J. Catalysis and Surface Science. *Phys. Today* **1999**, *52*, 32–38.
- (6) Kyriakou, G.; Boucher, M. B.; Jewell, A. D.; Lewis, E. A.; Lawton, T. J.; Baber, A. E.; Tierney, H. L.; Flytzani-Stephanopoulos, M.; Sykes, E. C. H. Isolated Metal Atom Geometries as a Strategy for Selective Heterogeneous Hydrogenations. *Science* **2012**, *335*, 1209–1212.
- (7) Sachtler, W. M. H. Chemisorption Complexes on Alloy Surfaces. *Catal. Rev.: Sci. Eng.* **1976**, *14*, 193–210.
- (8) Ruff, M.; Takehiro, N.; Liu, P.; Norskov, J. K.; Behm, R. J. Size-specific Chemistry on Bimetallic Surfaces: A Combined Experimental and Theoretical Study. *ChemPhysChem* **2007**, *8*, 2068–2071.
- (9) Gao, F.; Goodman, D. W. Pd-Au Bimetallic Catalysts: Understanding Alloy Effects from Planar Models and (Supported) Nanoparticles. *Chem. Soc. Rev.* **2012**, *41*, 8009–8020.
- (10) Ma, Y. S.; Diemant, T.; Bansmann, J.; Behm, R. J. The Interaction of CO with PdAg/Pd(111) Surface Alloys: A Case Study of Ensemble Effects on a Bimetallic Surface. *Phys. Chem. Chem. Phys.* **2011**, *13*, 10741–10754.
- (11) Mancera, L. A.; Behm, R. J.; Gross, A. Structure and Local Reactivity of PdAg/Pd(111) Surface Alloys. *Phys. Chem. Chem. Phys.* **2013**, *15*, 1497–1508.
- (12) Kovnir, K.; Armbrüster, M.; Teschner, D.; Venkov, T. V.; Szentmiklosi, L.; Jentoft, F. C.; Knop-Gericke, A.; Grin, Y.; Schlögl, R. In Situ Surface Characterization of the Intermetallic Compound PdGa: A Highly Selective Hydrogenation Catalyst. *Surf. Sci.* **2009**, *603*, 1784–1792.
- (13) Osswald, J.; Kovnir, K.; Armbrüster, M.; Giedigkeit, R.; Jentoft, R. E.; Wild, U.; Grin, Y.; Schlögl, R. Palladium-Gallium Intermetallic Compounds for the Selective Hydrogenation of Acetylene, Part II: Surface Characterization and Catalytic Performance. *J. Catal.* **2008**, *258*, 219–227.

(14) Borodzinski, A.; Bond, G. C. Selective Hydrogenation of Ethyne in Ethene-Rich Streams on Palladium Catalysts, Part 2: Steady-State Kinetics and Effects of Palladium Particle Size, Carbon Monoxide, and Promoters. *Catal. Rev.: Sci. Eng.* **2008**, *50*, 379–469.

(15) Prinz, J.; Gaspari, R.; Pignedoli, C. A.; Vogt, J.; Gille, P.; Armbrüster, M.; Brune, H.; Gröning, O.; Passerone, D.; Widmer, R. Isolated Pd Sites on the Intermetallic PdGa(111) and PdGa(−1−1−1) Model Catalyst Surfaces. *Angew. Chem., Int. Ed.* **2012**, *51*, 9339–9343.

(16) Norskov, J. K.; Bligaard, T.; Rossmeisl, J.; Christensen, C. H. Towards the Computational Design of Solid Catalysts. *Nat. Chem.* **2009**, *1*, 37–46.

(17) Gille, P.; Ziemer, T.; Schmidt, M.; Kovnir, K.; Burkhardt, U.; Armbrüster, M. Growth of Large PdGa Single Crystals from the Melt. *Intermetallics* **2010**, *18*, 1663–1668.

(18) Armbrüster, M.; Borrmann, H.; Wedel, M.; Prots, Y.; Giedigkeit, R.; Gille, P. Refinement of the Crystal Structure of Palladium Gallium (1:1), PdGa. *Z. Kristallogr.: New Cryst. Struct.* **2010**, *225*, 617–618.

(19) Rosenthal, D.; Widmer, R.; Wagner, R.; Gille, P.; Armbrüster, M.; Grin, Y.; Schlögl, R.; Gröning, O. Surface Investigation of Intermetallic PdGa(−1−1−1). *Langmuir* **2012**, *28*, 6848–6856.

(20) VandeVondele, J.; Krack, M.; Mohamed, F.; Parrinello, M.; Chassaing, T.; Hutter, J. QUICKSTEP: Fast and Accurate Density Functional Calculations Using a Mixed Gaussian and Plane Waves Approach. *Comput. Phys. Commun.* **2005**, *167*, 103–128.

(21) Perdew, J. P.; Burke, K.; Ernzerhof, M. Generalized Gradient Approximation Made Simple. *Phys. Rev. Lett.* **1997**, *78*, 1396–1396.

(22) Pickett, W. E. Pseudopotential Methods in Condensed Matter Applications. *Comput. Phys. Rep.* **1989**, *9*, 115–197.

(23) Hoffmann, F. M. Infrared Reflection-Absorption Spectroscopy of Adsorbed Molecules. *Surf. Sci. Rep.* **1983**, *3*, 107–192.

(24) Morkel, M.; Rupprechter, G.; Freund, H. J. Ultrahigh Vacuum and High-pressure Coadsorption of CO and H₂ on Pd-(111): A Combined SFG, TDS, and LEED Study. *J. Chem. Phys.* **2003**, *119*, 10853–10866.

(25) Tüshaus, M.; Berndt, W.; Conrad, H.; Bradshaw, A. M.; Persson, B. Understanding the Structure of High Coverage CO Adlayers. *Appl. Phys. A* **1990**, *51*, 91–98.

(26) Yudanov, I. V.; Sahnoun, R.; Neyman, K. M.; Rosch, N.; Hoffmann, J.; Schauer mann, S.; Johane k, V.; Unterhalt, H.; Rupprechter, G.; Libuda, J.; et al. CO Adsorption on Pd Nanoparticles: Density Functional and Vibrational Spectroscopy Studies. *J. Phys. Chem. B* **2003**, *107*, 255–264.

(27) Hammer, B.; Hansen, L. B.; Norskov, J. K. Improved Adsorption Energetics within Density-Functional Theory Using Revised Perdew-Burke-Ernzerhof Functionals. *Phys. Rev. B* **1999**, *59*, 7413–7421.

(28) Armbrüster, M.; Behrens, M.; Cinquini, F.; Föttinger, K.; Grin, Y.; Haghof er, A.; Klötzer, B.; Knop-Gericke, A.; Lorenz, H.; Ota, A.; et al. How to Control the Selectivity of Palladium-based Catalysts in Hydrogenation Reactions: The Role of Subsurface Chemistry. *ChemCatChem* **2012**, *4*, 1048–1063.

(29) Angyan, J.; Loos, M.; Mayer, I. Covalent Bond Orders and Atomic Valence Indexes in the Topological Theory of Atoms in Molecules. *J. Phys. Chem.* **1994**, *98*, 5244–5248.

(30) Krajci, M.; Hafner, J. Structure and Chemical Reactivity of the Polar Three-Fold Surfaces of GaPd: A Density-functional Study. *J. Chem. Phys.* **2013**, *138*, 124703.